Numerical simulation and analysis of the dark and illuminated *J–V* characteristics of a-Si-H p–i–n diodes

2006 J. Phys.: Condens. Matter 18 5459

(http://iopscience.iop.org/0953-8984/18/23/017)

INSTITUTE OF PHYSICS PUBLISHING JOURNAL OF PHYSICS: CONDENSED MATTER

J. Phys.: Condens. Matter **18** (2006) 5459–5471 doi:10.1088/0953-8984/18/23/017

Numerical simulation and analysis of the dark and illuminated J–V characteristics of a-Si-H p–i–n diodes

A M Meftah[1], **A F Meftah and A Merazga**

Laboratoire des Matériaux Semiconducteurs & Métalliques, Département de Physique, Université Mohammed Khieder, BP 145, Biskra 07000, Algeria

E-mail: amjad_meftah@yahoo.fr

Received 22 February 2006, in final form 4 May 2006
Published 26 May 2006
Online at stacks.iop.org/JPhysCM/18/5459

Abstract

Dark and illuminated current–voltage (J–V) characteristics of the hydrogenated amorphous silicon (a-Si:H) p–i–n diode have been simulated by solving numerically the full set of transport equations. The dependence of the dark current on the intrinsic layer (i-layer) thickness and on the measurement temperature is investigated by taking into account the presence of the p/i interface defect states. Good agreement with experimental data is obtained when the p/i interface defect density is increased with increasing i-layer thickness. Further, no appreciable influence was remarked for the i/n interface states on the J–V characteristic, which is in agreement with experimental observations. The numerical simulation also concerned the evaluation of the diode photo-parameters, i.e. the short-circuit current density (J_{sc}) and the open-circuit voltage (V_{oc}), and reproduced, in a good manner, the light intensity dependence of J_{sc} and V_{oc} for different i-layer thicknesses.

1. Introduction

In this paper, we discuss some transport proprieties of hydrogenated amorphous silicon (a-Si:H) p–i–n diodes, which characterize the electrical behaviour of these diodes under dark and light steady state conditions. a-Si:H p–i–n diodes are known for their cheap fabrication technology, the possibility of their deposition on large areas and their good optical absorption proprieties [1, 2]. Therefore, they are widely used as solar cells and photodetectors. a-Si:H is also known for its continuous density of states distribution in the mobility gap [3, 4] which plays a dominant role in the electric proprieties of a-Si:H p–i–n diodes. Several methods are employed to characterize these devices; measurements of the dark and illuminated current–voltage (J–V) characteristics present a relatively easy way to give information about the diode characteristics, and thus the quality of such devices [5–8]. Also, through computer simulation,

[1] Author to whom any correspondence should be addressed.

Table 1. Electrical parameters of the a-Si:H p–i–n diode used in the simulation.

$\varepsilon\varepsilon_0 = 1.0536 \times 10^{-12}$ F cm^{-1}	$E_{ap} = 0.47$ eV
$\mu_n = 20$ cm^2 V^{-1} s^{-1}	$E_{an} = 0.24$ eV
$\mu_p = 2$ cm^2 V^{-1} s^{-1}	$k_B T_c = 0.025$ eV
$D_{n,p} = \mu_{n,p} k_B T/q$	$k_B T_v = 0.048$ eV
$N_c = N_v = 2 \times 10^{20}$ cm^{-3}	$C_c = 5 \times 10^{-7}$ cm^3 s^{-1}
$E_g = 1.72$ eV	$C_n = 10^{-8}$ cm^3 s^{-1}
Parameters of dangling bond density of states according to the defect pool model [19]	
$N_{SiSi} = 2 \times 10^{23}$ cm^{-3}	$\sigma = 0.19$ eV
$H = 5 \times 10^{21}$ cm^{-3}	$T^* = 500$ K
$E_p = 1.25$ eV	$U = 0.2$ eV

we can understand, in a better way, the role of various parameters such as the thickness of the intrinsic layer (i-layer), the measurement temperature, and the density of gap states in the intrinsic and in the p/i interface layers, and then get an idea of the factors limiting the diode performance. The presence of the p/i interface defects has been demonstrated by several experimental measurements [9–12]. These defects can be due to the specific characteristic of the growth process, like the formation of a contaminated or a hydrogen-rich layer between the p and i materials. Moreover, Rothwarf [13] has suggested a mechanism based on the conversion of empty valence-band tail states into dangling bonds which justifies the presence of defects at a p/i junction even in the case of a homojunction. These defects have, therefore, an important role in determining the diode performances.

In this work, numerical simulations, using a transport model [14] extended to the studied situation, are performed in order to investigate the sensitivity of the dark J–V characteristic to two parameters, i-layer thickness and measurement temperature, taking into account the presence of the defect states at the interfaces. The obtained results are compared to the experimental measures of Matsuura *et al* [5]. Furthermore, the dependence of the short-circuit current (J_{sc}) and the open-circuit voltage (V_{oc}) on the light intensity for different thicknesses of the i-layer is carried out.

2. Simulation model

The a-Si:H p–i–n diode is considered here as a one-dimensional device for which the Poisson's equation and the two carrier continuity equations [15, 16, 14] are simultaneously solved, under steady state conditions, using the coupled method of Newton. The simulation is performed by taking into account the typical model of the a-Si:H gap density of states, which includes the band tail and dangling bond states [3, 4, 17, 18]. We also consider [14] the spatial distribution of the dangling bond density of states, which is calculated using the recent defect pool model of Powell and Deane [19]. In order to model the effects of the interface states, we have assumed a thin region in the i-layer next to the p/i (and i/n) interfaces with a high density of dangling bond states [20, 21], that is, we treat as 'interface states' those dangling bond states which are located in these regions. We attribute to these states capture coefficients which are identical to those used for the dangling bond states in the bulk of the i-layer.

Following Matsuura's parameters [5], thicknesses of the p and n layers have been fixed, respectively, at 100 and 200 Å, while the thickness of the i-layer was varied between 770 and 7600 Å. The remaining parameters used in the simulation are listed in table 1. Respectively, ε and ε_0 are the permittivities of the semiconductor and the vacuum, μ_n and μ_p are the electron

Table 2. Optical parameters used in the simulation.

$\phi = 10^{10}$–10^{17} cm^{-2} s^{-1}	$T_r = 0.9$
$\alpha = 10^5$ cm^{-1}	$R_f = 0.9$

and hole band mobilities, D_n and D_p are the electron and hole diffusion coefficients (cm^2 s^{-1}) related to the mobilities by the Einstein relation, N_c and N_v are the effective densities of states at the conduction (E_c) and valence (E_v) band edge energies, E_{ap} and E_{an} are the activation energies in the p- and n-type layers, T_c and T_v are the characteristic absolute temperatures of the conduction and valence band tail, C_c and C_n are the capture coefficients for the charged and neutral gap-states in both tails and mid-gap (dangling bond) states, and H and N_{SiSi} are the total density of hydrogen and the number of electrons in the silicon bonding states. Further, k_B is the Boltzmann constant, E_g is the mobility gap, E_p is the most probable energy in the distribution of the dangling bond density of states, σ is the width of the defect pool, T^* is the freezing temperature and U is the correlation energy. Moreover, the input electrical parameters (table 1) are adopted from the literature [22, 19] and not treated as fitting entities in order to make the model the most predictive possible. The dangling bond density of states, obtained with these parameters, has a value of about 2.5×10^{16} cm^{-3} in the middle of the i-layer.

Concerning the light conditions, the device is illuminated through the p layer by a monochromatic beam with a photon flux ϕ. The optical carrier generation rate G is calculated taking into account the transmittance T_r of the glass/TCO substrate and the reflectivity R_f of the n/metal contact. We neglect the reflection at the TCO/p contact. Then, G at the space coordinate x of the device is given by

$$G(x) = T_r \cdot \alpha \cdot \phi[\exp(-\alpha x) + R_f \exp(-\alpha(2d - x))] \tag{1}$$

where α is the absorption coefficient (cm^{-1}) and d the thickness of the device (cm).

The optical parameters used in the simulation are listed in table 2, where the values of T_r and R_f are taken from [20]. However, the flux ϕ is simply varied in order to simulate the variation of the light intensity.

Concerning the boundary conditions, we have assumed ideal Ohmic contacts, that is, at the semiconductor/metal interface, the carrier concentration in the semiconductor is assumed to be equal to that at equilibrium.

With all these conditions in hand, our numerical program yields the dark and illuminated J–V characteristics of the a-Si:H p–i–n diode, and also the spectral response if we consider the whole solar spectrum, although the study is restricted here to the case of monochromatic illumination.

3. Results and discussions

Figure 1(a) illustrates the i-layer thickness dependence of the simulated dark J–V characteristics at the room temperature ($T = 297.5$ K) which is compared to the measurements (figure 1(b)) of Matsuura *et al* [5]. Similarly, figure 2 gives the temperature dependence of the dark J–V characteristics in the simulated case (figure 2(a)) and the corresponding experimental one (figure 2(b)) [5]. Note that in this case the i-layer thickness is fixed at 2600 Å. Further, we have assumed the presence of a p/i interface layer with a surface density of defect states $N_{p/i}$, and a thickness $W_{p/i}$, the latter being fixed at $W_{p/i} = 29$ Å for all diodes. We can see, from these figures, that the simulation reproduces well the experimental tendencies. Indeed, the magnitude of the forward current (figure 1) is independent of the i-layer thickness in the range of low voltages where the current density J increases exponentially with the voltage.

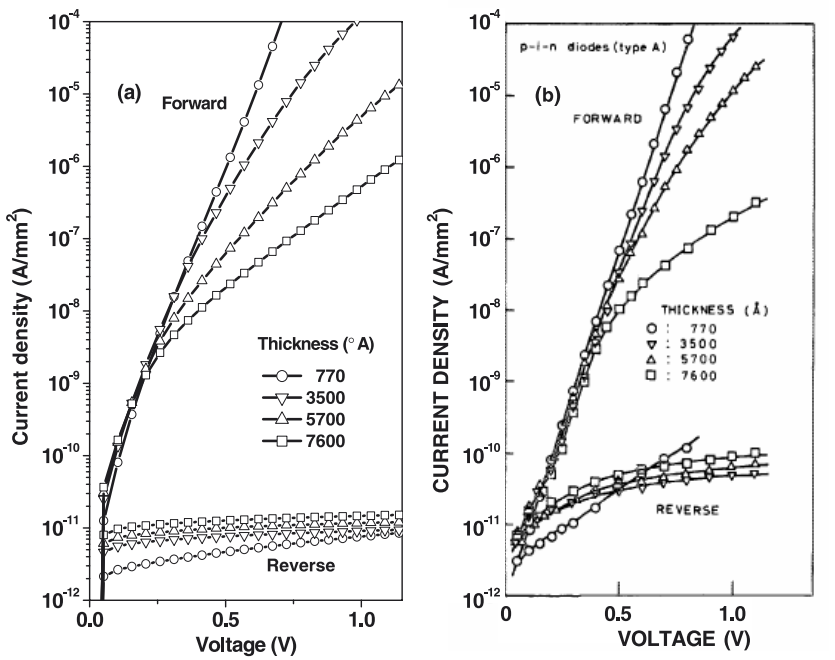

Figure 1. Dependence of the dark J–V characteristics on the i-layer thickness: (a) simulation; (b) measures [5] at room temperature.

In the other ranges, the forward current decreases with increasing i-layer thickness, while the reverse current increases over the whole considered range of voltage when the i-layer thickness increases. We point out that the dependence on the i-layer thickness observed experimentally, mainly for the reverse current, is obtained by the simulation when we assume an increase of the density of the p/i interface defect states ($N_{p/i}$) with increasing i-layer thickness. $N_{p/i}$ was increased by taking values of 5.2×10^{12}, 6.6×10^{12}, 8×10^{12} and 8.8×10^{12} cm^{-2} respectively for the corresponding values 770, 3500, 5700 and 7600 Å of the i-layer thickness. Moreover, the values of $N_{p/i}$ were chosen such that the simulated reverse current reaches the range of magnitudes found experimentally [5]. However, if we fix $N_{p/i}$ at the same value (for instance 5.2×10^{12} cm^{-2}) for all thicknesses, as shown in figure 3, no clear thickness dependence is discerned for the simulated reverse current. In fact, at low voltages, the dark currents obtained for the two thicknesses 5700 and 7600 Å are the lowest and have almost the same magnitude. By further increasing the applied voltage, the dark current of the thinnest diode (770 Å) increases rapidly and becomes the highest.

The increase of the i-layer thickness is obtained experimentally by the rise of the deposition time [5]. It is reasonable to expect that $N_{p/i}$ increases with the extension of the i-layer thickness; i.e., more time for the sample to be exposed to deposition factors (like substrate temperature, contact and exchange with plasma ... etc) can increase the defect density at the p/i interface. Therefore, it is of interest to look for the formation mechanisms of interface states, and then obtain their evolution with the deposition time.

To understand the origin of currents presented in figures 1, 2, we have used the Chen and Lee calculations [23], which allow us to represent the total density of current J as the sum of two components: the recombination current J_R and the drift/diffusion current J_D;

$$J = J_R + J_D. \tag{2}$$

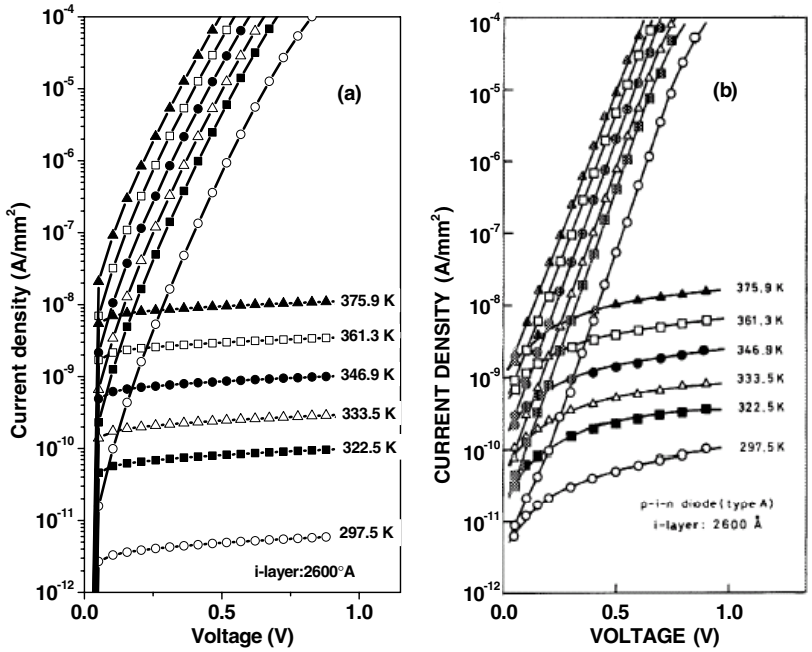

Figure 2. Temperature dependence of the dark J–V characteristics with i-layer of 2600 Å: (a) simulation; (b) measures [5].

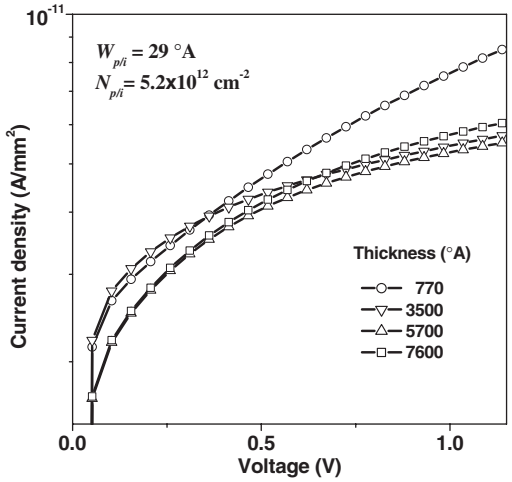

Figure 3. Reverse J–V characteristics computed for different i-layer thicknesses, with $N_{\mathrm{p/i}} = 5.2 \times 10^{12}$ cm^{-2} and $W_{\mathrm{p/i}} = 29$ Å at $T = 297.5$ K.

Figure 4 shows the variations of J_{R} and J_{D} together with the computed total current density J with the applied voltage for the four diodes. We can distinguish three regions: a region (I) at low voltages, where the total current is dominated by the recombination current J_{R} and is nearly independent of the i-layer thickness, then a region (II) at intermediate voltages; here J is still a recombination current but it decreases with increasing i-layer thickness; finally, a region

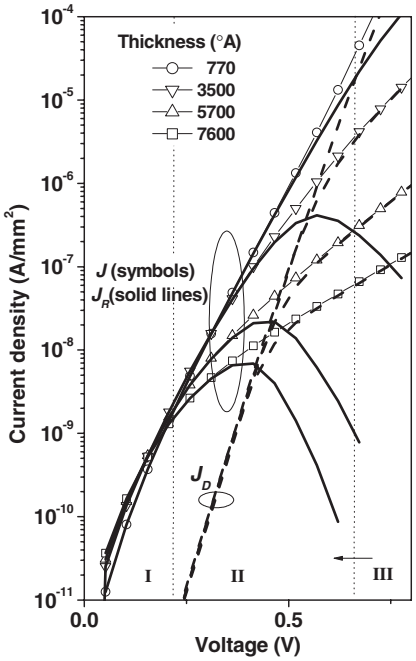

Figure 4. Applied voltage dependence of the total current density J, the recombination current J_{R} and the drift/diffusion current J_{D}, computed with varying i-layer thickness.

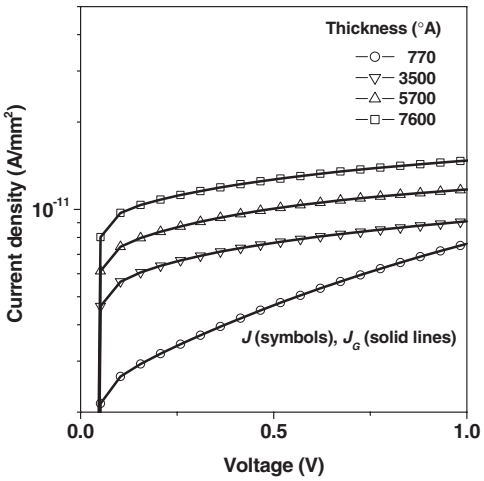

Figure 5. Total current density J and its thermal generation component J_{G}, as functions of the applied voltage, computed at reverse bias for different i-layer thicknesses.

(III) at high voltages, where the total current is dominated by the drift/diffusion current J_{D} and also decreases with increasing i-layer thickness. The width of regions (II) and (III) depends on the i-layer thickness; when the latter increases, region (II) narrows, leading to widening of region (III).

At reverse bias, we have a thermal generation mechanism of free carriers from localized states instead of a recombination process; the total reverse current J is then expected to be

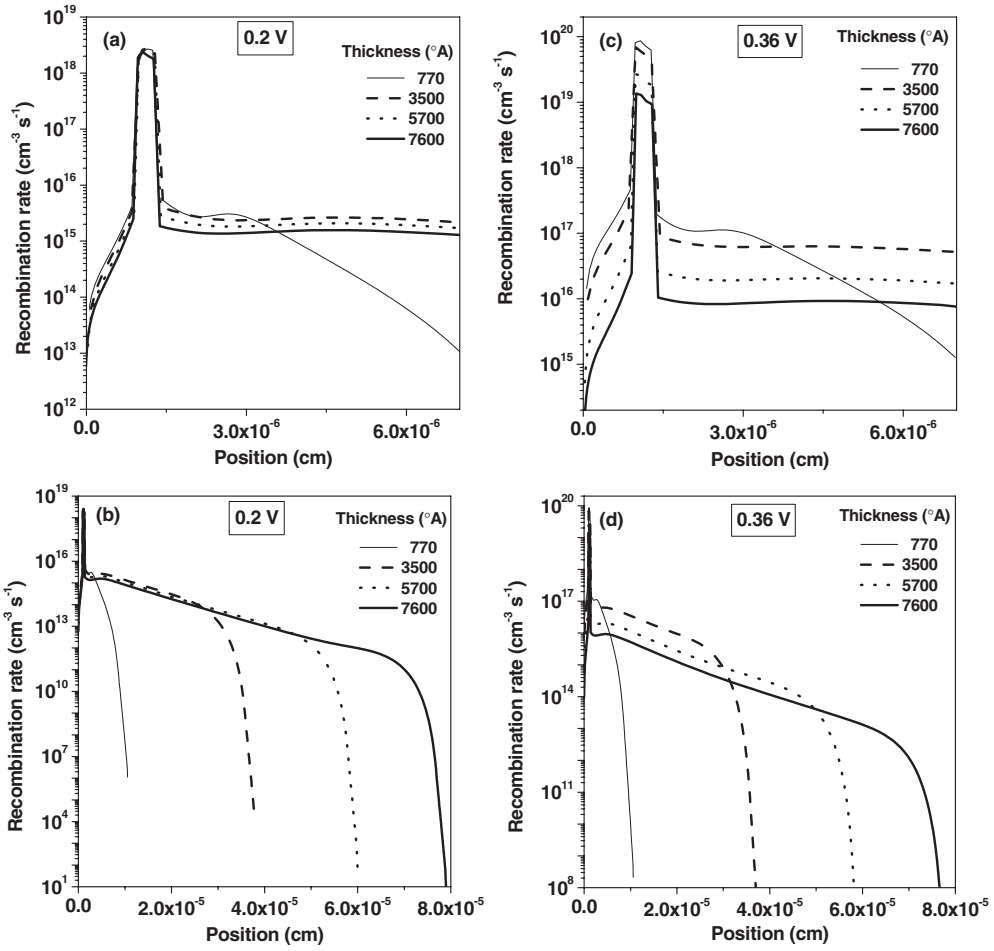

Figure 6. Recombination rate as a function of position: (a) over the p/i interface layer and (b) over the whole p–i–n diode under a forward bias voltage of 0.2 V, (c) over the p/i interface layer and (d) over the whole p–i–n diode under a forward bias voltage of 0.36 V, with varying i-layer thickness.

dominated by the thermal generation current J_G, which is effectively verified by simulation as shown in figure 5.

To explain the independence of the forward current J on the i-layer thickness, observed at low voltages, we present, in figure 6, the recombination rate, as a function of position, under a forward bias voltage of 0.2 V (figures 6(a) and (b)) and of 0.36 V (figures 6(c) and (d)). The first voltage value (0.2 V) belongs to region (I) of figure 4, while the second one (0.36 V) is in region (II). In cases (a) and (c) of the figure, we illustrate the recombination rate profiles over the p/i interface layer, and in cases (b) and (d) the profiles are plotted over the whole p–i–n diode. The different curves correspond to the different thicknesses of the i-layer. It is clear, according to this figure, that the recombination rate is dominated by the recombination at the p/i interface layer. At 0.2 V (figures 6(a) and (b)), the recombination rate is seen to saturate to nearly the same value for all the diodes, either in the interface layer or in the bulk of the i-layer. Since the interface layer is the dominant region for recombination, we can expect, from figure 6(a), that the forward current, which is a recombination current in this case, will be independent of the

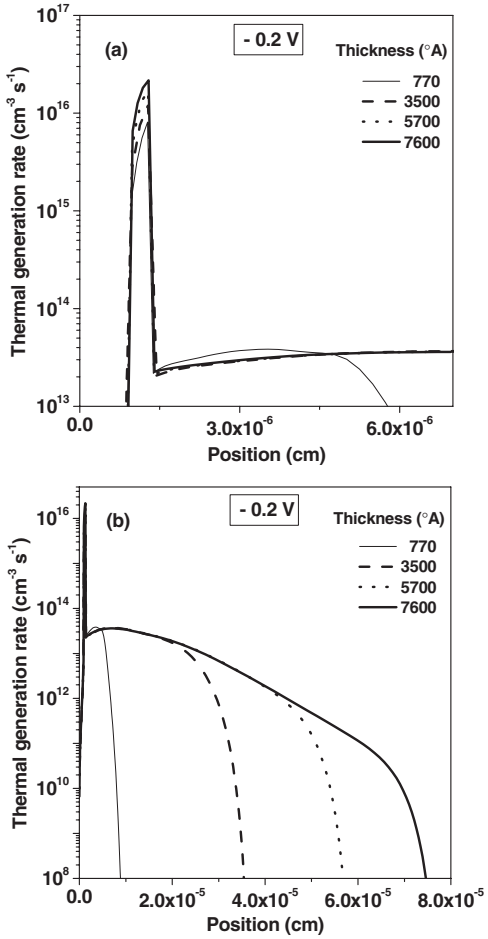

Figure 7. Thermal generation rate as a function of position: (a) over the p/i interface layer and (b) over the whole p–i–n diode, under a reverse bias voltage of −0.2 V, with varying i-layer thickness.

i-layer thickness. However, at 0.36 V, as shown in figures 6(c) and (d), the value to which the recombination rate saturates, either in the interface layer or in the bulk of the i-layer, decreases as the p–i–n diode becomes thicker, then a decrease of the forward current is expected.

At reverse bias voltage, as shown in figures 7(a) and (b) for −0.2 V, the thermal generation rate, for the four thicknesses, saturates to nearly the same value in the bulk of the i-layer (figure 7(b)); however, its maximum, in the p/i interface layer, increases when the i-layer thickness increases, leading, thus, to increasing of the reverse current.

In figure 8 is plotted the electric field intensity distribution over the p/i interface layer (figure 8(a)), and over the whole p–i–n diode (figure 8(b)), under a forward bias voltage of 0.82 V; this voltage value belongs to region (III) of figure 4 where the current is dominated by the drift/diffusion current J_D. The signs (−) and (+) in the figure indicate the regions where the electric field is negative or positive, respectively. For the four diodes, the electric field increases significantly at the interfaces with a peak value of $\sim 8 \times 10^4$–2.6×10^5 V cm^{-1} at the p/i interface, and of ~ 1.4–1.5×10^5 V cm^{-1} at the i/n one. This large interface field is

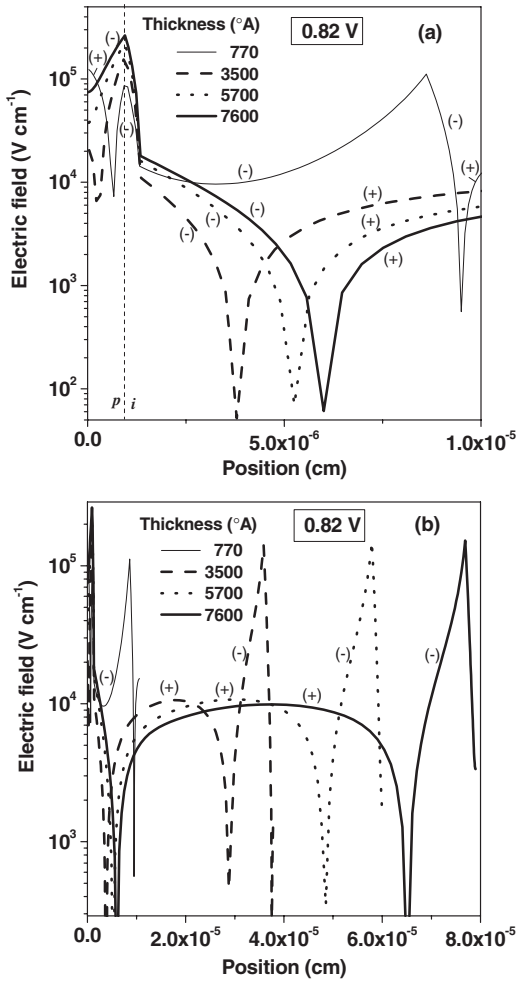

Figure 8. Electric field intensity distribution: (a) over the p/i interface layer and (b) over the whole p–i–n diode, under a forward bias voltage of 0.82 V, for different i-layer thicknesses.

caused by the high space charge density, at the interfaces, due to (1) the heavily doped p and n layers, (2) the spatial variation of the dangling bond density of states distribution, which means more defect states at the interfaces compared to the i-layer bulk, and (3) the presence of the p/i interface defect states. One points out that the variation of the electric field at the p/i interface (relative to the i/n one) is more appreciable because of the increasing of the $N_{\mathrm{p/i}}$ density as the i-layer thickness increases. In the middle of the i-layer, the electric field reaches nearly the same value for all diodes, which is $\sim 10^4$ V cm^{-1}. However, it is negative along the whole i-layer of the thinnest diode. This means that the depletion regions, resulting from the p/i and i/n interfaces, are still overlapped under a forward bias voltage of 0.82 V. In this case, free carriers, injected from the p- and n-sides, will diffuse into the i-layer against the negative internal field, and they can (as they cannot) reach the opposite contact. This depends on which one of the two mechanisms (recombination or diffusion) dominates the transport. Effectively, returning to figure 4, we can see that, for the thinnest diode, the recombination dominates at voltages $V < 0.6$ V, which means that most carriers do not traverse the i-layer but recombine via

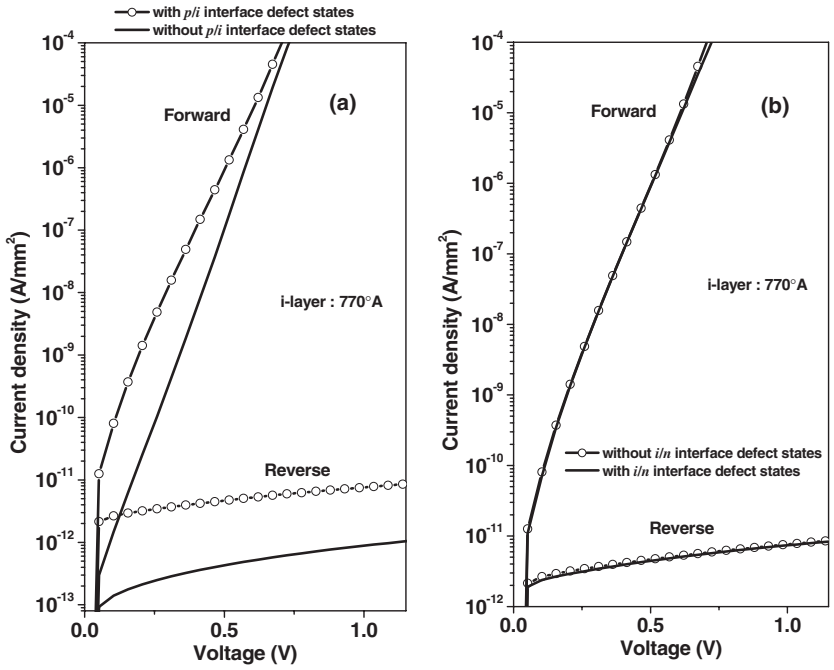

Figure 9. Computed J–V characteristics (symbols) compared to the two cases: (a) there are no p/i interface defect states, (b) assuming the presence of both p/i and i/n interface defect states, with i-layer of 770 Å, $N_{\mathrm{p/i}} = 5.2 \times 10^{12}$ cm^{-2}, $N_{\mathrm{i/n}} = 4 \times 10^{12}$ cm^{-2} and $W_{\mathrm{p/i}} = 29$ Å.

dangling bonds in order to support the transport. With increasing the forward bias voltage from 0.6 V, the contribution of recombination is reduced, leaving room for diffusion to dominate; in this case the carriers can reach the opposite contact only by diffusion. For the other diodes (figure 8), we can see that, under the same value of the applied voltage, the electric field changes its direction in the bulk of the i-layer and becomes positive. This means that the depletion regions are well separated to give a positive field in this region. Now, drift of carriers will dominate in the i-layer. Indeed, after their diffusion from the doped regions, the carriers will find a positive field, which drifts them through the i-layer to the opposite contact. The total current will be then controlled by the two mechanisms (drift and diffusion).

To illustrate more clearly the effect of the p/i interface defect states, we plot, in figure 9, the dark J–V characteristic computed with the presence of these states, compared to the two cases of J–V characteristic: (a) assuming the absence of the p/i interface states (figure 9(a)); (b) in addition to their presence, we assume the presence of the i/n interface defect states (figure 9(b)). Plotted curves are for the thinnest diode (770 Å) with $N_{\mathrm{p/i}} = 5.2 \times 10^{12}$ cm^{-2} and $W_{\mathrm{p/i}} = 29$ Å. We assume that the p/i and i/n interface layers have the same thickness. Since the n-layer is thinner than the i-layer, the i/n interface will be exposed (during the deposition process) to factors that create interface states for a time shorter than the one during which the p/i interface defects are created. Then, the surface density, $N_{\mathrm{i/n}}$, of defect states at the i/n interface is expected to be lower than $N_{\mathrm{p/i}}$. We have chosen $N_{\mathrm{i/n}} = 4 \times 10^{12}$ cm^{-2} (figure 9(b)). As shown in case (a) of the figure, the p/i interface defects cause an appreciable increase of the reverse current over the whole range of the applied voltage. The forward current, however, increases significantly in the region where it is dominated by recombination. Effectively, these currents are more sensitive to such parameters. From figure 9(b), we can see that there is no significant

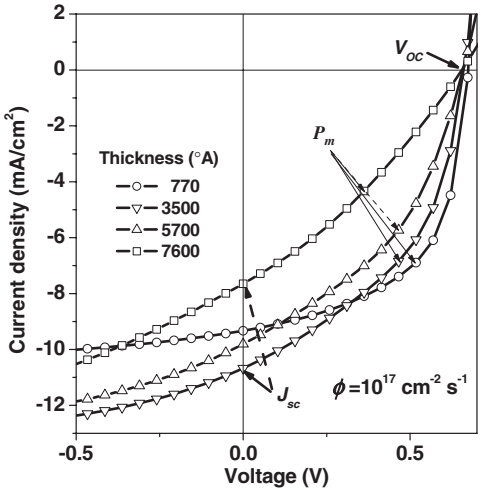

Figure 10. Illuminated J–V characteristics calculated for different thicknesses of the i-layer, with photon flux of 10^{17} cm^{-2} s^{-1} and temperature $T = 297.5$ K.

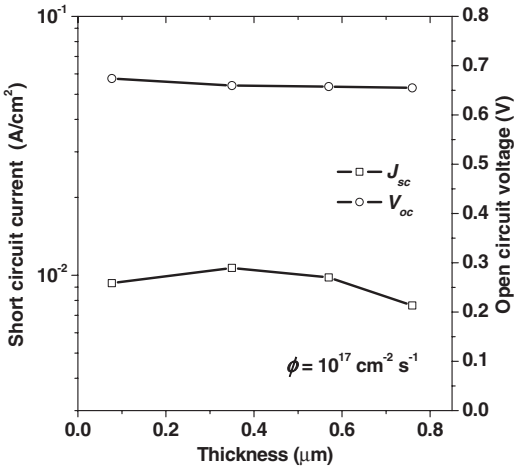

Figure 11. Short-circuit current density, J_{sc}, and the open-circuit voltage, V_{oc}, versus the i-layer thickness with $\phi = 10^{17}$ cm^{-2} s^{-1} and $T = 297.5$ K.

effect resulting from the presence of the i/n interface layer. This leads to the conclusion that the current is more influenced by the p/i interface state rather than the i/n one, which is in agreement with the experimental result notified on such diodes [5].

After analysing the dark behaviour of the considered p–i–n diodes, which presents the essential aim of this work, some results concerned with the illumination case are now presented. As mentioned previously, we assume a monochromatic illumination which creates a non-uniform photogeneration rate along the device (equation (1)). Figure 10 shows the calculated J–V characteristics under illumination with a photon flux $\phi = 10^{17}$ cm^{-2} s^{-1} (see table 2 for the remaining parameters). The different curves correspond to the different thicknesses of the i-layer at $T = 297.5$ K. As shown, the illuminated J–V characteristic is characterized by its 'open-circuit voltage', V_{oc}, which is the value of the voltage V for which the current

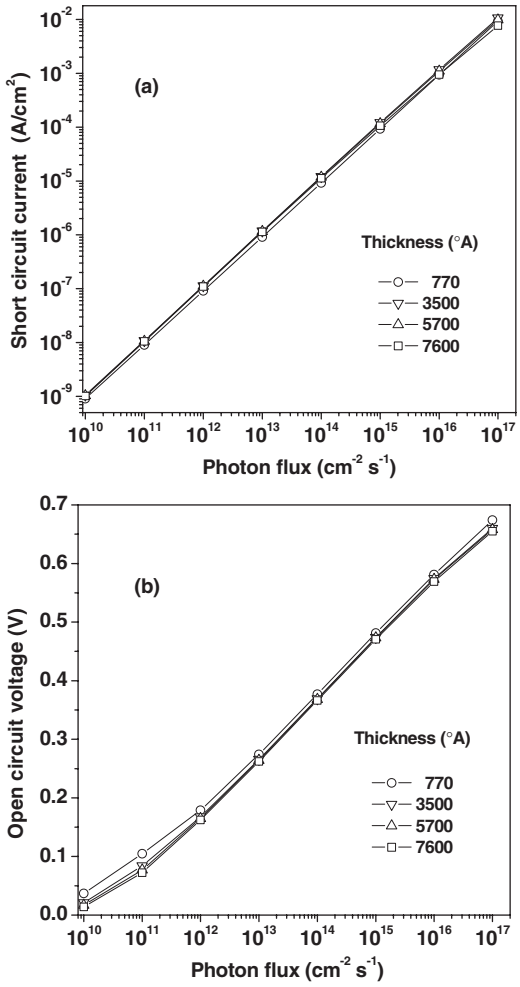

Figure 12. (a) Short-circuit current, J_{sc}, and (b) the open-circuit voltage, V_{oc}, as functions of the photon flux, with varying i-layer thickness.

density $J = 0$, and the 'short-circuit current density', J_{sc}, which is the magnitude of the current density at which $V = 0$ V. Under short-circuit or open-circuit conditions, no power is delivered to the external circuit. When the voltage across the diode rises from 0 V to V_{oc}, a power density $P(V) = -J(V) \cdot V$ is delivered to the external circuit. The voltage–current pairs corresponding to the maximum power P_m are indicated in the figure. In figure 11, J_{sc} and V_{oc} are plotted against the i-layer thickness. We can see, from these figures, that there is practically no dependence of J_{sc} and V_{oc} on the i-layer thickness. Figure 12 shows the J_{sc} and V_{oc} as functions of the photon flux ϕ. This figure clearly indicates an increase of J_{sc} and V_{oc} with rising light intensity for all diodes. However, we can discern, at low intensities (figure 12(b)), a slight decrease of V_{oc} with increasing i-layer thickness. The dependence of J_{sc} on the photon flux ϕ (figure 12(a)) possesses the form of $J_{sc} \sim \phi^{\gamma}$, where $\gamma \sim 0.99$, which means a linear current–flux relation. The diodes work, thus, normally as solar cells. The obtained behaviours of J_{sc} and V_{oc} are similar to what was observed experimentally [5, 6]. No device optimization is performed in the current paper but we envisage making this work the topic of a next paper.

4. Conclusion

The behaviour of the dark and illuminated J–V characteristics of the a-Si:H p–i–n diodes has been analysed by numerical simulation. We have investigated the dependence of the dark current on the i-layer thickness and on the measurement temperature by taking into account the presence of the p/i interface defect states. The simulation results have been compared to the experimental measures of Matsuura *et al* [5]. A good agreement is obtained when we assume an increase of the p/i interface defect density when the i-layer thickness increases. Moreover, computations performed have allowed us to give some explanations on the origin and the behaviour of dark currents. Recombination has been found to dominate the forward current at low and intermediate voltages. However, at high voltages it is the drift/diffusion component which predominates. At reverse bias, the current is limited by the thermal generation mechanism over the whole range of the applied voltage. By analysing the interface defect effects, we have shown that the current is more influenced by the p/i interface states rather than those of the i/n one, which is similar to experimental observations [5]. Simulations for the illumination case of the a-Si:H p–i–n diode show behaviours similar to what was observed experimentally [5, 6]: (1) practically, there is no effect of the i-layer thickness on the J_{sc} and V_{oc}; (2) a dependence is obtained for J_{sc} and V_{oc} on the light intensity as expected for the solar cells.

References

[1] Cody G D, Abeles B, Wronski C R, Stephens C R and Brooks B 1980 *Sol. Cells* **2** 227
[2] Zollonds J H 2001 Electronic characterisation and computer modelling of thin film materials and devices for optoelectronic applications *PhD Thesis* University of Abertay, Dundee
[3] Street R A 1991 *Hydrogenated Amorphous Silicon* ed R A Street (Cambridge: Cambridge University Press)
[4] Stutzmann M 1989 *Phil. Mag.* B **60** 531
[5] Matsuura H, Matsuda A, Okushi H and Tanaka K 1985 *J. Appl. Phys.* **58** 1578
[6] Kroon M A and van Swaaij R A C M M 2001 *J. Appl. Phys.* **90** 994
[7] Tchakarov S, Roca i Cabarrocas P, Dutta U, Chatterjee P and Equer B 2003 *J. Appl. Phys.* **94** 7317
[8] Deng J, Pearce J M, Koval R J, Vlahos V, Collins R W and Wronski C R 2003 *Appl. Phys. Lett.* **82** 3023
[9] de Seta M, Fiorini P, Evangelisti F and Armigliato A 1989 *Superlatt. Microstruct.* **5** 149
[10] Asano A, Ichimura T, Uchida Y and Sakai H 1988 *J. Appl. Phys.* **63** 2346
[11] Murthy R V R, Dutta V and Singh S P 1994 *J. Appl. Phys.* **33** L1581
[12] Dutta V and Murthy R V R 1997 *J. Appl. Phys.* **36** 6687
[13] Rothwarf A 1988 *Proc. 20th IEEE Photovoltaic Specialist Conf.* (New York: IEEE)
[14] Meftah A M, Meftah A F, Hiouani F and Merazga A 2004 *J. Phys.: Condens. Matter* **16** 2003
[15] Kurata M 1982 *Numerical Analysis for Semiconductor Devices* (Lexington, MA: Heath)
[16] Selberherr S 1984 *Analysis and Simulation of Semiconductor Devices* (Berlin: Springer)
[17] Cohen M H, Fritzsche H and Ovshinsky S R 1969 *Phys. Rev. Lett.* **22** 1065
[18] Mott N F 1970 *Phil. Mag.* **22** 7
[19] Powell M J and Deane S C 1996 *Phys. Rev.* B **53** 10121
[20] Tasaki H, Kim W Y, Hallerdt M, Konagai M and Takahashi K 1988 *J. Appl. Phys.* **63** 550
[21] Mittiga A, Fiorini P, Falconieri M and Evangelisti F 1989 *J. Appl. Phys.* **66** 2667
[22] Klimovsky E, Rath J K, Schropp R E I and Rubinelli F A 2002 *Thin Solid Films* **422** 211
[23] Chen I and Lee S 1982 *J. Appl. Phys.* **53** 1045